Report

Current Biology

The Occipital Place Area Is Causally Involved in Representing Environmental Boundaries during Navigation

Highlights

- TMS to the OPA impairs accuracy of navigation to locations in a virtual arena
- This impairment is observed for locations defined by distance to a bounding wall
- This impairment is *not* found for locations defined by landmarks or visual markings
- Results causally implicate OPA in the perception of environmental boundaries

Authors

Joshua B. Julian, Jack Ryan, Roy H. Hamilton, Russell A. Epstein

Correspondence

jjulian@sas.upenn.edu

In Brief

Julian et al. use transcranial magnetic stimulation to establish a causal role for the occipital place area (OPA) in the perception of environmental boundaries. Stimulation of the OPA impairs navigation to remembered locations—but only when these locations are defined by reference to environmental boundaries, not landmarks or non-boundary features.

Julian et al., 2016, Current Biology *26*, 1104–1109
April 25, 2016
http://dx.doi.org/10.1016/j.cub.2016.02.066

CellPress

CellPress

Current Biology
Report

The Occipital Place Area Is Causally Involved in Representing Environmental Boundaries during Navigation

Joshua B. Julian,[1,*] Jack Ryan,[1] Roy H. Hamilton,[2] and Russell A. Epstein[1]
[1]Department of Psychology, University of Pennsylvania, Philadelphia, PA 19104, USA
[2]Department of Neurology, University of Pennsylvania, Philadelphia, PA 19104, USA
*Correspondence: jjulian@sas.upenn.edu
http://dx.doi.org/10.1016/j.cub.2016.02.066

SUMMARY

Thirty years of research suggests that environmental boundaries—e.g., the walls of an experimental chamber or room—exert powerful influence on navigational behavior, often to the exclusion of other cues [1–9]. Consistent with this behavioral work, neurons in brain structures that instantiate spatial memory often exhibit firing fields that are strongly controlled by environmental boundaries [10–15]. Despite the clear importance of environmental boundaries for spatial coding, however, a brain region that mediates the perception of boundary information has not yet been identified. We hypothesized that the occipital place area (OPA), a scene-selective region located near the transverse occipital sulcus [16], might provide this perceptual source by extracting boundary information from visual scenes during navigation. To test this idea, we used transcranial magnetic stimulation (TMS) to interrupt processing in the OPA while subjects performed a virtual-reality memory task that required them to learn the spatial locations of test objects that were either fixed in place relative to the boundary of the environment or moved in tandem with a landmark object. Consistent with our prediction, we found that TMS to the right OPA impaired spatial memory for boundary-tethered, but not landmark-tethered, objects. Moreover, this effect was found when the boundary was defined by a wall, but not when it was defined by a marking on the ground. These results show that the OPA is causally involved in boundary-based spatial navigation and suggest that the OPA is the perceptual source of the boundary information that controls navigational behavior.

RESULTS

In experiment 1, we tested the causal role of the occipital place area (OPA) in boundary-based navigation by using transcranial magnetic stimulation (TMS) to interrupt processing in the OPA while participants (n = 12) learned the locations of four test objects inside a virtual arena (Supplemental Experimental Procedures). Following the behavioral paradigm pioneered by Doeller and colleagues, on each trial subjects saw a word denoting one of the test objects and indicated its location by navigating to it from a random start location and making a button-press response (the "replace" phase; Figure 1A) [11]. Participants were then teleported to a random position and the object appeared in its correct location and was collected (the "feedback" phase). The arena was limited by a circular boundary wall and contained a rotationally symmetric landmark object; it was also surrounded by distal cues (mountains and sky, rendered at infinity). Thus, the distal cues could be used to determine heading, but locations within the arena could only be defined based on distances to the bounding wall or the landmark object.

A set of 16 trials (four per experimental object) composed a block, and there were three blocks in the experiment. Critically, the landmark object was moved relative to the boundary between blocks 1 and 2 and again between blocks 2 and 3. Two test objects maintained their locations relative to the boundary after these moves and two maintained their locations relative to the landmark (Figure 1B). Within and across blocks, participants learned the relationships between object locations and the landmark or boundary by using the feedback provided. This design allowed us to assess learning of object location relative to each cue independently. Prior to each block, we applied continuous theta burst TMS (cTBS; three-pulse bursts at 50 Hz repeated every 200 ms for 40 s) [17] to either the right OPA or a vertex control site (Supplemental Experimental Procedures; Figure S1A). Each subject received stimulation to both TMS sites in two sessions separated by 1 week, with stimulation order counterbalanced across subjects. The OPA was functionally defined in each subject based on fMRI data obtained in a separate experimental session.

We focused on the OPA as a potential source for the boundary signal because it is one of three brain regions that respond selectively in fMRI during the visual perception of scenes (e.g., landscapes, streets, and rooms) [16, 18–21]. We conjectured that this scene-preferential response might be driven in part by analysis of boundary surfaces, as the presence of such surfaces is one of the primary characteristics that distinguish scenes from non-preferred stimuli such as single objects and faces [22, 23]. Previous fMRI work has shown sensitivity to boundaries in the two other scene-responsive regions—the parahippocampal place area (PPA) and retrosplenial complex (RSC)—but several aspects of the literature suggest that these regions might not

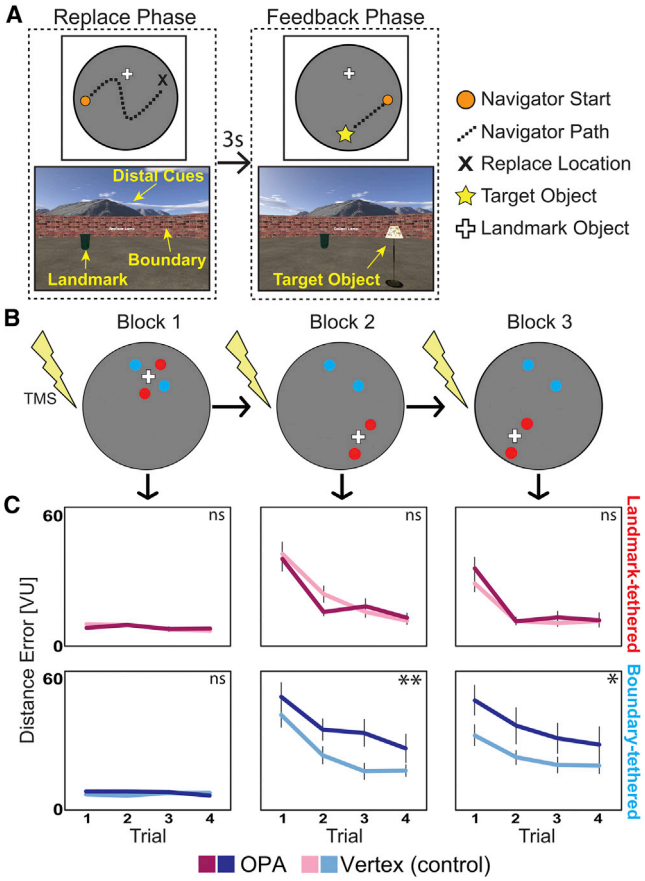

Figure 1. Experiment 1 Methods and Results

(A) Trial structure (after initial learning of object locations in block 1; see the Supplemental Experimental Procedures). On each trial, participants navigated to the remembered location of the target object ("replace" phase) and, after a short delay with a black screen, received feedback ("feedback" phase). The top shows a map of the virtual trajectory taken by the participant on each phase of a typical trial, and the bottom shows example views of the virtual environment from the participant's perspective. The name of the target object remained on the center of the screen during the entire trial.

(B) Participants learned four object locations over three blocks. The landmark was moved relative to the boundary at the start of block 2, and again at the start of block 3. Two objects were tethered to the landmark (red dots) and two objects were tethered the boundary (blue dots). TMS was applied to either the OPA or a vertex control site prior to the start of each block.

(C) The top row shows the average distance error for the landmark-tethered objects (in red), and the bottom row shows the average distance error for the boundary-tethered object (in blue) during the replace phase. Vertex sessions are in light colors, and OPA sessions are in dark colors. Distance error is the distance between the replace location and the correct location for each trial, averaged over the two objects paired with each cue, in virtual units (VU). Compared to vertex, participants were significantly impaired at replacing the boundary objects after OPA stimulation, but not the landmark objects. Significance markers indicate the strength of the difference between OPA and vertex for each object type and block (one-tailed t test; $^{**}p < 0.01$, $^{*}p < 0.05$). Error bars indicate ±1 SEM.

See also Figure S1 and Table S1.

be the ultimate source of the boundary signal. In particular, although the PPA responds to the presence of boundaries [24, 25] and represents the shape of the space as defined by boundaries [26, 27], it is also sensitive to non-boundary scene elements that are useful for place recognition such as surface textures and landmark objects [28–31]. Similarly, the RSC codes location and heading relative to boundaries [32] and the spatial extent of the bounded space in a scene [33]; however, the RSC is believed to play a primarily mnemonic role in spatial navigation and thus is unlikely to be the source of the perceptual boundary signal [34, 35]. In contrast, the function of OPA is believed to be perceptual, thus making it a more likely candidate.

Performance during experiment 1 was assessed by measuring the distance between each object's replaced location and the correct location (Figure 1C). We analyzed data from block 1 separately from the data from blocks 2 and 3, as the critical distinction between boundary-tethered and landmark-tethered objects is not made until the later blocks. In block 1, a 2 × 2 × 4 ANOVA with factors for stimulation site (OPA versus vertex), object type (boundary tethered versus landmark tethered), and trial (1–4) found no effects of stimulation site ($F(1,11) = 0.15$, $p = 0.71$) and—as expected by design—no effect of object type ($F(1,11) = 0.02$, $p = 0.90$). There was marginal improvement in performance across trials ($F(3,33) = 2.65$, $p = 0.07$, $\eta_p^2 = 0.19$) as a result of the feedback. Performance was noticeably better in this block than in subsequent blocks, which is not surprising because in block 1 participants could use both the boundary and the landmark as references to code the location of each target object and there was no conflict between these two cues.

We next assessed performance during blocks 2–3, in which the relative movement of the boundary and landmark caused the two cues to indicate different locations. In this case, we conducted an analogous ANOVA with block (2–3) as an additional factor, summarized in Table S1 and below. There was a main effect of object type ($F(1,11) = 7.09$, $p = 0.02$, $\eta_p^2 = 0.39$), with greater error for the boundary- than landmark-tethered objects, and a main effect of stimulation site ($F(1,11) = 14.76$, $p = 0.003$, $\eta_p^2 = 0.57$), with greater error during the OPA than vertex sessions. Critically, there was a significant interaction between stimulation site and object type ($F(1,11) = 10.14$, $p = 0.009$, $\eta_p^2 = 0.48$): compared to vertex, participants were significantly impaired when replacing the boundary-tethered objects ($t(11) = 3.80$, $p = 0.003$; all pairwise tests two-tailed unless otherwise noted), but there was no difference in performance between stimulation sites for the landmark-tethered objects ($t(11) = 0.23$, $p = 0.82$). Thus, consistent with our predictions, TMS to the OPA specifically impaired the ability to navigate to locations defined by reference to boundaries. This impairment could reflect a deficit in perceiving boundaries during the encoding stage of each trial, the retrieval stage, or both.

The specific impairment for boundary-tethered objects after OPA stimulation was not due to the task being inherently more difficult for these objects: performance levels did not differ significantly between the boundary- and landmark-tethered objects during the vertex sessions ($t(11) = 1.77$, $p = 0.11$). Nor was it due to an impairment in sensitivity to feedback in general: there was no interaction between stimulation site and trial ($F(3,9) = 1.13$, $p = 0.35$) or block ($F(1,11) = 0.54$, $p = 0.48$). Nor was it due to a speed-accuracy trade-off: there was no interaction between stimulation site and object type in response time (RT) during the replace or feedback phases (both $F(1,11)$s < 1.0, both ps > 0.34; Figure S1C). Path length and path tortuosity were also both matched between stimulation sites, indicating

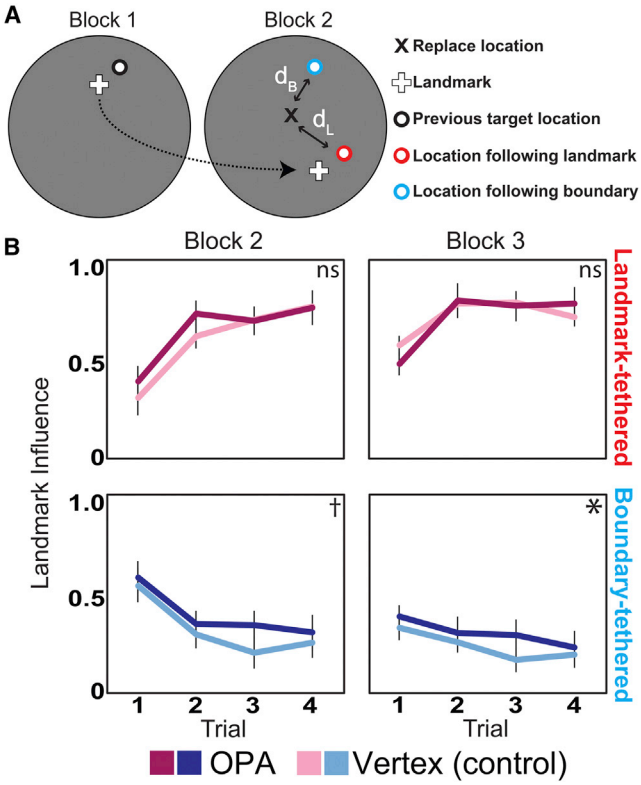

Figure 2. Influence of the Landmark on Replace Locations in Experiment 1

(A) The relative influence of the landmark was calculated as d_B / (d_L + d_B), where d_L is the distance of the response from the target location previously associated with the landmark and d_B is the distance of the response from the target location previously associated with the boundary. This measure ranges from 0 to 1, where 0 is complete influence of the boundary and 1 is complete influence of the landmark. For block 3, two target locations were associated with the boundary for landmark-tethered objects, one from block 1 and the other from block 2, and so we used the location associated with the lowest d_B.

(B) The top row shows the relative influence of the landmark on landmark-tethered objects (in red), and the bottom row shows the relative influence of the landmark on boundary-tethered objects (in blue). Vertex sessions are in light colors, and OPA sessions are in dark colors. Over the course of each block and trial, participants became more likely to use the landmark to localize landmark-tethered objects and less likely to use the landmark to localize boundary-tethered objects. Compared to vertex, participants were more likely to be influenced by the landmark after OPA stimulation. Significance markers indicate the strength of the difference between OPA and vertex for each object type and block (one-tailed t test; *$p < 0.05$, $^{\dagger}p < 0.09$). Error bars indicate ±1 SEM.

See also Figure S1 and Table S1.

that the motor and planning aspects of the task were unimpaired by TMS to the OPA (both F(1,11)s < 1.35, both ps > 0.27; Figure S1C). Thus, subjects performed the task in the same manner after OPA stimulation and learned at a similar rate, but their ability to use boundary information for spatial memory was reduced, consistent with a boundary-specific perceptual deficit.

During blocks 2–3, the landmark and boundary predict conflicting target object locations. If boundary information is perceived as less reliable after OPA stimulation, then OPA stimulation may cause a bias to use the landmark to replace the target objects. To examine whether performance errors could be explained in part by over-reliance on the landmark, we computed the relative influence of the landmark on the replace locations during blocks 2–3 (Figure 2A). A 2 × 2 × 2 × 4 ANOVA with factors for stimulation site, object type, block, and trial revealed increasing landmark influence on the landmark-tethered objects and decreasing landmark influence on the boundary-tethered objects across blocks ($F(1,11) = 12.81$; $p = 0.004$, $\eta_p^2 = 0.54$) and trials ($F(3,33) = 27.76$; $p < 0.001$, $\eta_p^2 = 0.72$) (Figure 2B; see also Table S1). Thus, participants learned the associations between the target objects and the appropriate cue. Importantly, however, the landmark had greater influence during the OPA than the vertex sessions ($F(1,11) = 6.45$; $p = 0.03$, $\eta_p^2 = 0.37$), indicating a shift toward use of the landmark after OPA stimulation. This shift was found for the boundary-tethered objects ($t(11) = 2.60$, $p = 0.03$), but not the landmark-tethered objects ($t(11) = 0.23$, $p = 0.55$), although the interaction between object type and stimulation site was not significant ($F(1,11) = 1.01$; $p = 0.34$). Notably, overall landmark influence during the vertex sessions was significantly correlated across participants with the magnitude of the boundary-specific memory impairment during the OPA-stimulation sessions ($r^2 = 0.72$, $p < 0.001$; Figure S1B). Thus, when the OPA is disrupted, subjects are more likely to use the landmark to localize the objects, despite the fact that this is an inappropriate reference for the boundary-tethered objects; moreover, this increase in landmark influence is greatest in subjects who are already most inclined to use the landmark. These results are consistent with previous work indicating that the neural systems that mediate boundary- and landmark-based navigation interact with one another to guide spatial behavior [11, 36].

What information about boundaries does the OPA encode? There are at least two possibilities. First, the boundary and landmark differ in their physical structure: the boundary is an extended surface, whereas the landmark is discrete object. Second, the boundary takes up a larger retinotopic extent than the landmark. It is possible that the OPA codes large-scale visual information, rather than boundaries specifically. Indeed, previous studies have reported that the OPA has a peripheral visual bias [20, 37]. To distinguish between these alternatives, we ran a second experiment in which participants (n = 12) learned the locations of objects inside two distinct circular arenas using the same replace/feedback trial structure as in experiment 1 (Figure 1A). The first arena was surrounded by a wall as in experiment 1 (“wall arena”), whereas the second had no wall but consisted of a visual texture (or “mat”) drawn on the ground (“mat arena”) (Figure 3A; Supplemental Experimental Procedures). The two arenas had the same diameter, were visually identical except for the presence of the surface boundary, and were surrounded by the same distal orientational cues, rendered at infinity. Unlike in the wall arena, participants could walk outside the edges of the mat; thus, the edge of the mat did not provide a “boundary” in the sense of being a bounding surface that obstructed movement, though it did provide a reference for localizing the object. In contrast to experiment 1, there was no landmark object present, so in this case participants had to rely exclusively on the arena edge to determine target object position. For each arena, all trials (three for each object; 12 total) were presented within a single block, with arena order counterbalanced across participants. (Participants were also tested in

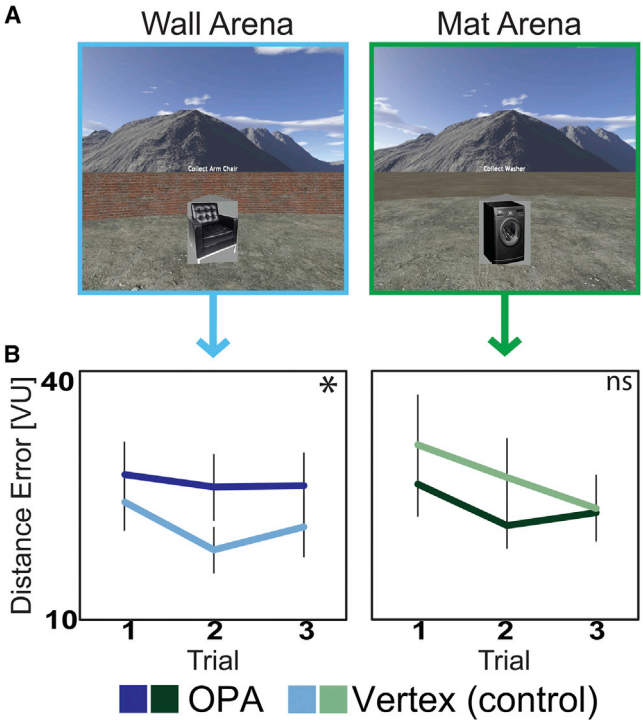

Figure 3. Experiment 2 Methods and Results

(A) Example views of the virtual environment from the participant's perspective during the feedback phase. There were two virtual arenas: one in which the arena was bounded by a wall (wall arena), and one in which the arena was bounded by a marking on the ground (mat arena). To ensure that all objects equally obscured the edges of the arenas, the target objects in experiment 2 were five-sided polyhedrons of the same height with images of the objects textured on the polyhedron's sides.

(B) Average distance error in virtual units (VU) in each arena, plotted separately for OPA (dark colors) and vertex (light colors) sessions. Stimulation to the right OPA impaired performance in the wall arena, but not in the mat arena. Significance markers indicate the strength of the difference between OPA and vertex for each Arena (one-tailed t test; *$p < 0.05$). Error bars indicate ±1 SEM. See also Figure S2 and Table S2.

a third arena in which the boundary was defined by a water barrier that blocked movement but results from this condition were inconclusive; see the Supplemental Experimental Procedures.) Prior to each block, we applied cTBS to either the functionally defined right OPA or a vertex control site (Figure S2A). Each subject received stimulation to both TMS sites in two sessions separated by 1 week with stimulation order counterbalanced across subjects.

A 2 × 2 × 3 ANOVA, with factors for stimulation site (OPA versus vertex), arena (wall versus mat), and trial (1–3), revealed no main effects of arena type ($F(1,11) = 0.12$, $p = 0.63$) or stimulation site ($F(1,11) = 0.25$, $p = 0.74$) but did reveal improvement of performance across trials ($F(2,10) = 5.48$, $p = 0.01$, $\eta_p^2 = 0.33$) (Figure 3B; see also Table S2). Critically, there was a significant interaction between arena and stimulation site ($F(1,11) = 5.97$, $p = 0.03$, $\eta_p^2 = 0.35$): OPA stimulation significantly impaired performance in the wall arena relative to vertex ($t(11) = 2.36$, $p = 0.04$), replicating the results of experiment 1 but did not significantly affect performance in the mat arena ($t(11) = 1.17$, $p = 0.27$). Control analyses further found that the wall-selective impairment after OPA stimulation was not due to (1) an impairment in overall sensitivity to feedback, as there was no interaction between stimulation site and trial (Figure 3B), nor (2) an interaction between arena type and stimulation site in RT (Figure S2C), nor (3) an effect of stimulation site on path length or path tortuosity (Figure S2C) (all Fs < 0.89, all ps > 0.35). Thus, stimulation of the OPA disrupts coding of locations relative to bounding surfaces, but not relative to large-scale visual information generally. Moreover, the fact that stimulation of the OPA impaired performance on the wall arena even though no landmark was present implies that OPA stimulation impairs the quality of the boundary representation itself, rather than simply causing a bias to rely on non-boundary cues.

DISCUSSION

Our results indicate that the OPA is causally involved in the coding of object locations relative to environmental surface boundaries. Stimulation of the OPA impaired accurate navigation to boundary-tethered, but not landmark-tethered, objects in experiment 1. Furthermore, this impairment was only observed in experiment 2 when the boundary of the arena was defined by a wall, not when it was defined by a marking on the ground.

These findings have important implications for our understanding of the neural basis of spatial navigation. There is extensive behavioral evidence that boundaries are a very salient navigational cue [1–9], and boundary-related spatial coding has been identified in several brain structures, including the hippocampal formation [10–15, 38] and RSC [32]. However, the perceptual source of this boundary information has remained a mystery. Our results suggest that the OPA may be that perceptual source. This conclusion dovetails with recent findings that the OPA is sensitive to "sense" (left/right) and distance information in visual scenes [39, 40] and is involved in making spatial judgments about object locations [41]. Moreover, the fact that stimulation of the OPA does *not* disrupt memory for locations defined by a marking on the ground is consistent with previous observations that the navigation system that codes locations relative to environmental geometry is often insensitive to large-scale non-boundary features [42, 43].

Although the precise connectivity of the OPA remains unknown, there are at least two possible pathways by which this boundary information might be communicated to the network of brain regions implicated in spatial navigation. First, the OPA and PPA are functionally connected [44, 45], and the PPA may serve as an intermediate input to the hippocampal formation [46, 47]. Second, the OPA may provide boundary information to the adjacent posterior parietal cortex, which projects to the RSC, PPA, and hippocampus [44, 48]. It also remains possible that the current results might be obtained by the use of a view-matching strategy in which the views are defined exclusively by boundaries, but not other visual features. In this case, a connection between the OPA and the broader navigational system would not be required. However, we think that this explanation is unlikely, as previous work suggests that people solve similar tasks by coding object location relative to boundaries, not by view matching [9].

In addition to demonstrating that the OPA is critical for boundary-based navigation, our results also provide insight into the

functional organization of the human visual system. The OPA forms a central node in the cortical network for scene perception, along with the PPA and RSC, and previous fMRI and TMS research has highlighted the importance of the OPA in scene-specific processing [16, 49–52]. Compared to the PPA and RSC, however, the precise function of the OPA has been less well explored. By implicating the OPA in the perception of environmental boundaries, our results suggest a potential function for this region that might explain its preferential response to scenes; namely, the OPA may respond selectively to scenes because such stimuli tend to depict navigational boundaries.

These results raise an important set of new questions regarding the function of the OPA in boundary-based navigation. First, is the OPA only involved in the *perception* of surface boundaries, or does it also serve a mnemonic function, both of which would have been disrupted by TMS in the present experiments? Although we prefer a perceptual account, we cannot rule out a mnemonic role for the OPA based on the current data alone. Second, does the OPA encode explicit representations of bounding geometry, or does it merely extract mid-level visual features that allow boundary representations to be constructed by downstream regions? Third, is the OPA involved in the coding of non-surface navigational barriers? We attempted to address this third question in experiment 2, but the results were inconclusive (see the Supplemental Experimental Procedures). We suspect that the OPA may be involved in the coding a wide range of environmental features that define the navigational affordances of local space, not just surface boundaries, but this remains to be established.

SUPPLEMENTAL INFORMATION

Supplemental Information includes Supplemental Experimental Procedures, two figures, and two tables and can be found with this article online at http://dx.doi.org/10.1016/j.cub.2016.02.066.

AUTHOR CONTRIBUTIONS

Conceptualization, J.B.J. and R.A.E.; Methodology, J.B.J., J.R., R.H.H., and R.A.E.; Software, J.B.J. and J.R.; Formal Analysis, J.B.J. and J.R.; Investigation, J.B.J. and J.R.; Resources, J.B.J., J.R., and R.H.H.; Writing – Original Draft, J.B.J. and R.A.E.; Writing – Review & Editing, J.B.J., R.H.H., and R.A.E.; Visualization, J.B.J., J.R., and R.A.E.; Supervision, R.H.H. and R.A.E.; Funding Acquisition, R.A.E.

ACKNOWLEDGMENTS

This work was supported by NIH (R01 EY-022350) and NSF (SBE-0541957) grants to R.A.E. and an NSF Graduate Research Fellowship to J.B.J. All participants provided informed consent in accordance with the Institutional Review Board of the University of Pennsylvania.

Received: January 13, 2016
Revised: February 24, 2016
Accepted: February 26, 2016
Published: March 24, 2016

REFERENCES

1. Cheng, K. (1986). A purely geometric module in the rat's spatial representation. Cognition *23*, 149–178.
2. Wang, R., and Spelke, E. (2002). Human spatial representation: insights from animals. Trends Cogn. Sci. *6*, 376–382.
3. Gallistel, C.R. (1990). The Organization of Learning (The MIT Press).
4. Doeller, C.F., and Burgess, N. (2008). Distinct error-correcting and incidental learning of location relative to landmarks and boundaries. Proc. Natl. Acad. Sci. USA *105*, 5909–5914.
5. Cheng, K., Huttenlocher, J., and Newcombe, N.S. (2013). 25 years of research on the use of geometry in spatial reorientation: a current theoretical perspective. Psychon. Bull. Rev. *20*, 1033–1054.
6. Julian, J.B., Keinath, A.T., Muzzio, I.A., and Epstein, R.A. (2015). Place recognition and heading retrieval are mediated by dissociable cognitive systems in mice. Proc. Natl. Acad. Sci. USA *112*, 6503–6508.
7. Hayward, A., McGregor, A., Good, M.A., and Pearce, J.M. (2003). Absence of overshadowing and blocking between landmarks and the geometric cues provided by the shape of a test arena. Q. J. Exp. Psychol. B *56*, 114–126.
8. McGregor, A., Horne, M.R., Esber, G.R., and Pearce, J.M. (2009). Absence of overshadowing between a landmark and geometric cues in a distinctively shaped environment: a test of Miller and Shettleworth (2007). J. Exp. Psychol. Anim. Behav. Process. *35*, 357–370.
9. Hartley, T., Trinkler, I., and Burgess, N. (2004). Geometric determinants of human spatial memory. Cognition *94*, 39–75.
10. O'Keefe, J., and Burgess, N. (1996). Geometric determinants of the place fields of hippocampal neurons. Nature *381*, 425–428.
11. Doeller, C.F., King, J.A., and Burgess, N. (2008). Parallel striatal and hippocampal systems for landmarks and boundaries in spatial memory. Proc. Natl. Acad. Sci. USA *105*, 5915–5920.
12. Krupic, J., Bauza, M., Burton, S., Barry, C., and O'Keefe, J. (2015). Grid cell symmetry is shaped by environmental geometry. Nature *518*, 232–235.
13. Lever, C., Burton, S., Jeewajee, A., O'Keefe, J., and Burgess, N. (2009). Boundary vector cells in the subiculum of the hippocampal formation. J. Neurosci. *29*, 9771–9777.
14. Solstad, T., Boccara, C.N., Kropff, E., Moser, M.-B., and Moser, E.I. (2008). Representation of geometric borders in the entorhinal cortex. Science *322*, 1865–1868.
15. Stewart, S., Jeewajee, A., Wills, T.J., Burgess, N., and Lever, C. (2014). Boundary coding in the rat subiculum. Philos. Trans. R. Soc. Lond. B Biol. Sci. *369*, 20120514.
16. Dilks, D.D., Julian, J.B., Paunov, A.M., and Kanwisher, N. (2013). The occipital place area is causally and selectively involved in scene perception. J. Neurosci. *33*, 1331–6a.
17. Huang, Y.-Z., Edwards, M.J., Rounis, E., Bhatia, K.P., and Rothwell, J.C. (2005). Theta burst stimulation of the human motor cortex. Neuron *45*, 201–206.
18. Grill-Spector, K. (2003). The neural basis of object perception. Curr. Opin. Neurobiol. *13*, 159–166.
19. Hasson, U., Harel, M., Levy, I., and Malach, R. (2003). Large-scale mirror-symmetry organization of human occipito-temporal object areas. Neuron *37*, 1027–1041.
20. Levy, I., Hasson, U., Harel, M., and Malach, R. (2004). Functional analysis of the periphery effect in human building related areas. Hum. Brain Mapp. *22*, 15–26.
21. Nakamura, K., Kawashima, R., Sato, N., Nakamura, A., Sugiura, M., Kato, T., Hatano, K., Ito, K., Fukuda, H., Schormann, T., and Zilles, K. (2000). Functional delineation of the human occipito-temporal areas related to face and scene processing. A PET study. Brain *123*, 1903–1912.
22. Epstein, R. (2005). The cortical basis of visual scene processing. Vis. Cogn. *12*, 954–978.
23. Henderson, J.M., and Hollingworth, A. (1999). High-level scene perception. Annu. Rev. Psychol. *50*, 243–271.
24. Epstein, R., and Kanwisher, N. (1998). A cortical representation of the local visual environment. Nature *392*, 598–601.
25. Committeri, G., Galati, G., Paradis, A.-L., Pizzamiglio, L., Berthoz, A., and LeBihan, D. (2004). Reference frames for spatial cognition: different brain

areas are involved in viewer-, object-, and landmark-centered judgments about object location. J. Cogn. Neurosci. *16*, 1517–1535.

26. Kravitz, D.J., Peng, C.S., and Baker, C.I. (2011). Real-world scene representations in high-level visual cortex: it's the spaces more than the places. J. Neurosci. *31*, 7322–7333.
27. Park, S., Brady, T.F., Greene, M.R., and Oliva, A. (2011). Disentangling scene content from spatial boundary: complementary roles for the parahippocampal place area and lateral occipital complex in representing real-world scenes. J. Neurosci. *31*, 1333–1340.
28. Cant, J.S., and Xu, Y. (2012). Object ensemble processing in human anterior-medial ventral visual cortex. J. Neurosci. *32*, 7685–7700.
29. Harel, A., Kravitz, D.J., and Baker, C.I. (2013). Deconstructing visual scenes in cortex: gradients of object and spatial layout information. Cereb. Cortex *23*, 947–957.
30. Vass, L.K., and Epstein, R.A. (2013). Abstract representations of location and facing direction in the human brain. J. Neurosci. *33*, 6133–6142.
31. Schinazi, V.R., and Epstein, R.A. (2010). Neural correlates of real-world route learning. Neuroimage *53*, 725–735.
32. Marchette, S.A., Vass, L.K., Ryan, J., and Epstein, R.A. (2014). Anchoring the neural compass: coding of local spatial reference frames in human medial parietal lobe. Nat. Neurosci. *17*, 1598–1606.
33. Park, S., Konkle, T., and Oliva, A. (2015). Parametric coding of the size and clutter of natural scenes in the human brain. Cereb. Cortex *25*, 1792–1805.
34. Epstein, R.A. (2008). Parahippocampal and retrosplenial contributions to human spatial navigation. Trends Cogn. Sci. *12*, 388–396.
35. Vann, S.D., Aggleton, J.P., and Maguire, E.A. (2009). What does the retrosplenial cortex do? Nat. Rev. Neurosci. *10*, 792–802.
36. Poldrack, R.A., Clark, J., Paré-Blagoev, E.J., Shohamy, D., Creso Moyano, J., Myers, C., and Gluck, M.A. (2001). Interactive memory systems in the human brain. Nature *414*, 546–550.
37. Levy, I., Hasson, U., Avidan, G., Hendler, T., and Malach, R. (2001). Center-periphery organization of human object areas. Nat. Neurosci. *4*, 533–539.
38. Bird, C.M., Capponi, C., King, J.A., Doeller, C.F., and Burgess, N. (2010). Establishing the boundaries: the hippocampal contribution to imagining scenes. J. Neurosci. *30*, 11688–11695.
39. Dilks, D.D., Julian, J.B., Kubilius, J., Spelke, E.S., and Kanwisher, N. (2011). Mirror-image sensitivity and invariance in object and scene processing pathways. J. Neurosci. *31*, 11305–11312.
40. Persichetti, A.S., and Dilks, D.D. (2016). Perceived egocentric distance sensitivity and invariance across scene-selective cortex. Cortex *77*, 155–163.
41. Nasr, S., Devaney, K.J., and Tootell, R.B. (2013). Spatial encoding and underlying circuitry in scene-selective cortex. Neuroimage *83*, 892–900.
42. Lee, S.A., Spelke, E.S., and Vallortigara, G. (2012). Chicks, like children, spontaneously reorient by three-dimensional environmental geometry, not by image matching. Biol. Lett. *8*, 492–494.
43. Lee, S.A., and Spelke, E.S. (2011). Young children reorient by computing layout geometry, not by matching images of the environment. Psychon. Bull. Rev. *18*, 192–198.
44. Baldassano, C., Beck, D.M., and Fei-Fei, L. (2013). Differential connectivity within the parahippocampal place area. Neuroimage *75*, 228–237.
45. Rafique, S.A., Solomon-Harris, L.M., and Steeves, J.K. (2015). TMS to object cortex affects both object and scene remote networks while TMS to scene cortex only affects scene networks. Neuropsychologia *79* (Pt A), 86–96.
46. Naber, P.A., Caballero-Bleda, M., Jorritsma-Byham, B., and Witter, M.P. (1997). Parallel input to the hippocampal memory system through peri- and postrhinal cortices. Neuroreport *8*, 2617–2621.
47. Ho, J.W., and Burwell, R.D. (2014). Perirhinal and Postrhinal Functional Inputs to the Hippocampus. In Space, Time and Memory in the Hippocampal Formation, D. Derdikman, and J.J. Knierim, eds. (Springer), pp. 55–81.
48. Kravitz, D.J., Saleem, K.S., Baker, C.I., and Mishkin, M. (2011). A new neural framework for visuospatial processing. Nat. Rev. Neurosci. *12*, 217–230.
49. Nasr, S., Liu, N., Devaney, K.J., Yue, X., Rajimehr, R., Ungerleider, L.G., and Tootell, R.B. (2011). Scene-selective cortical regions in human and nonhuman primates. J. Neurosci. *31*, 13771–13785.
50. Bettencourt, K.C., and Xu, Y. (2013). The role of transverse occipital sulcus in scene perception and its relationship to object individuation in inferior intraparietal sulcus. J. Cogn. Neurosci. *25*, 1711–1722.
51. Marchette, S.A., Vass, L.K., Ryan, J., and Epstein, R.A. (2015). Outside Looking In: Landmark Generalization in the Human Navigational System. J. Neurosci. *35*, 14896–14908.
52. Ganaden, R.E., Mullin, C.R., and Steeves, J.K. (2013). Transcranial magnetic stimulation to the transverse occipital sulcus affects scene but not object processing. J. Cogn. Neurosci. *25*, 961–968.

Current Biology, Volume *26*

Supplemental Information

The Occipital Place Area Is Causally Involved in Representing Environmental Boundaries during Navigation

Joshua B. Julian, Jack Ryan, Roy H. Hamilton, and Russell A. Epstein

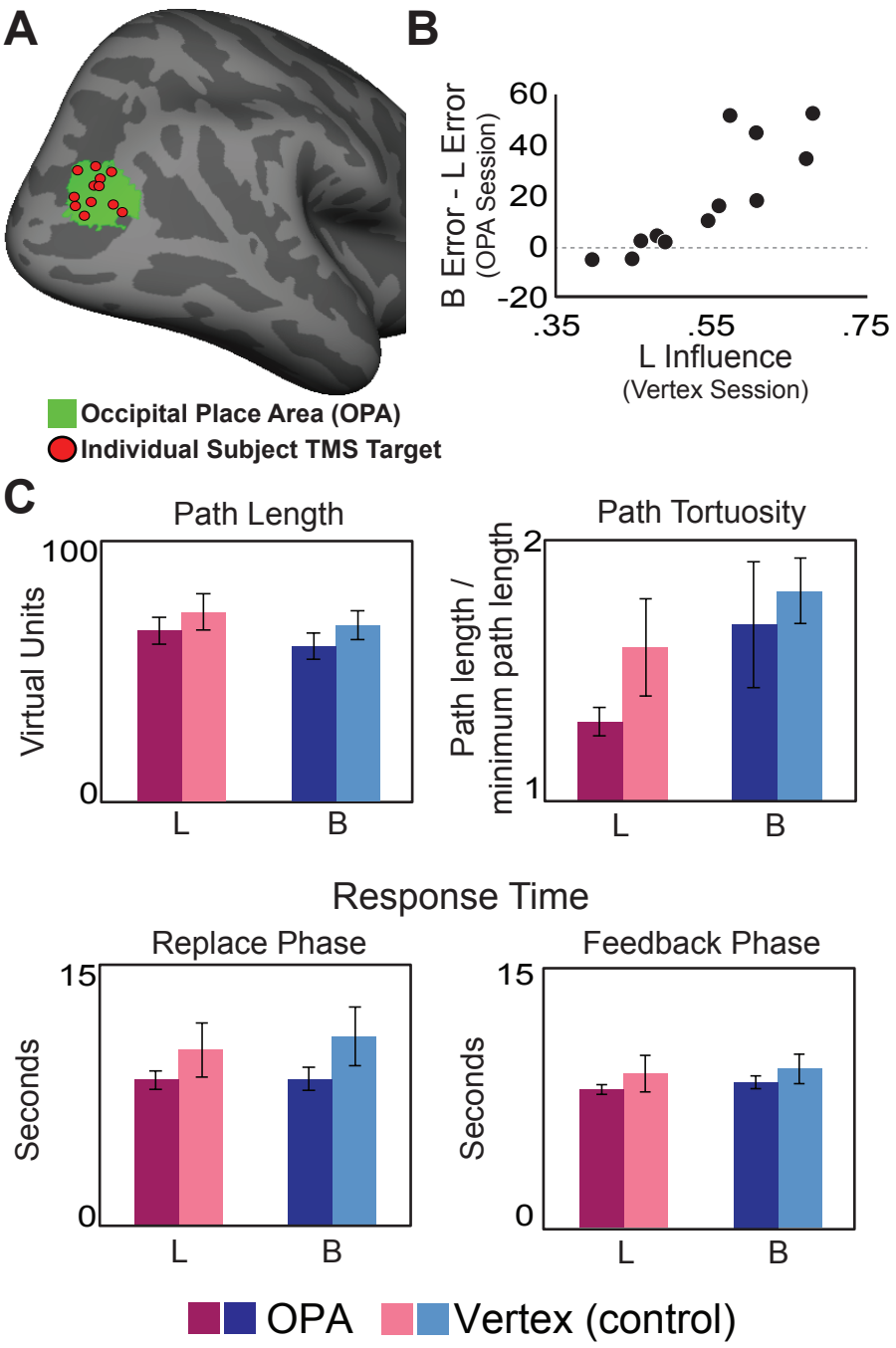

Figure S1. Supplemental Methods and Results for Experiment 1 (related to Figures 1 and 2). **A)** The group-based right Occipital Place Area (OPA) derived from a large number (42) of subjects across several studies from our laboratory, shown in green on the average cortical surface [S1]. The OPA TMS target site was defined for each participant as the OPA voxel exhibiting peak scene-selectivity. Each red dot denotes an OPA target site for a single participant in Experiment 1 (mean Talairach coordinates: [34, -77, 21]). **B**) Correlation between overall landmark influence during the Vertex session and boundary-specific memory impairment (i.e., boundary-tethered object distance error minus landmark-tethered object distance error) during the OPA session across participants. **C**) Mean path length and path tortuosity during the replace phase, and mean response time during both the replace phase and feedback phase, separately for the OPA (dark colors) and Vertex (light colors) sessions for the landmark- (*L*; in red) and boundary-related (*B*; in blue) objects (±1 SEM). Path tortuosity for each trial was computed as the path length divided by the Euclidean distance between the starting and end location of the path taken by the participant. Separate 2(object type: landmark-tethered vs. boundary-tethered) x 2(stimulation site: OPA vs. Vertex) ANOVAs revealed no significant main effects or interactions for path length, or response time during the replace or feedback phases (all $F(1,11)$s < 2.25, all ps > 0.1). Path tortuosity was marginally lower for the landmark-tethered than boundary-tethered objects ($F(1,11) = 4.15$, p=0.07), but critically there was no significant main effect of stimulation site or interaction (both $F(1,11)$s < 1.35, both ps > 0.27).

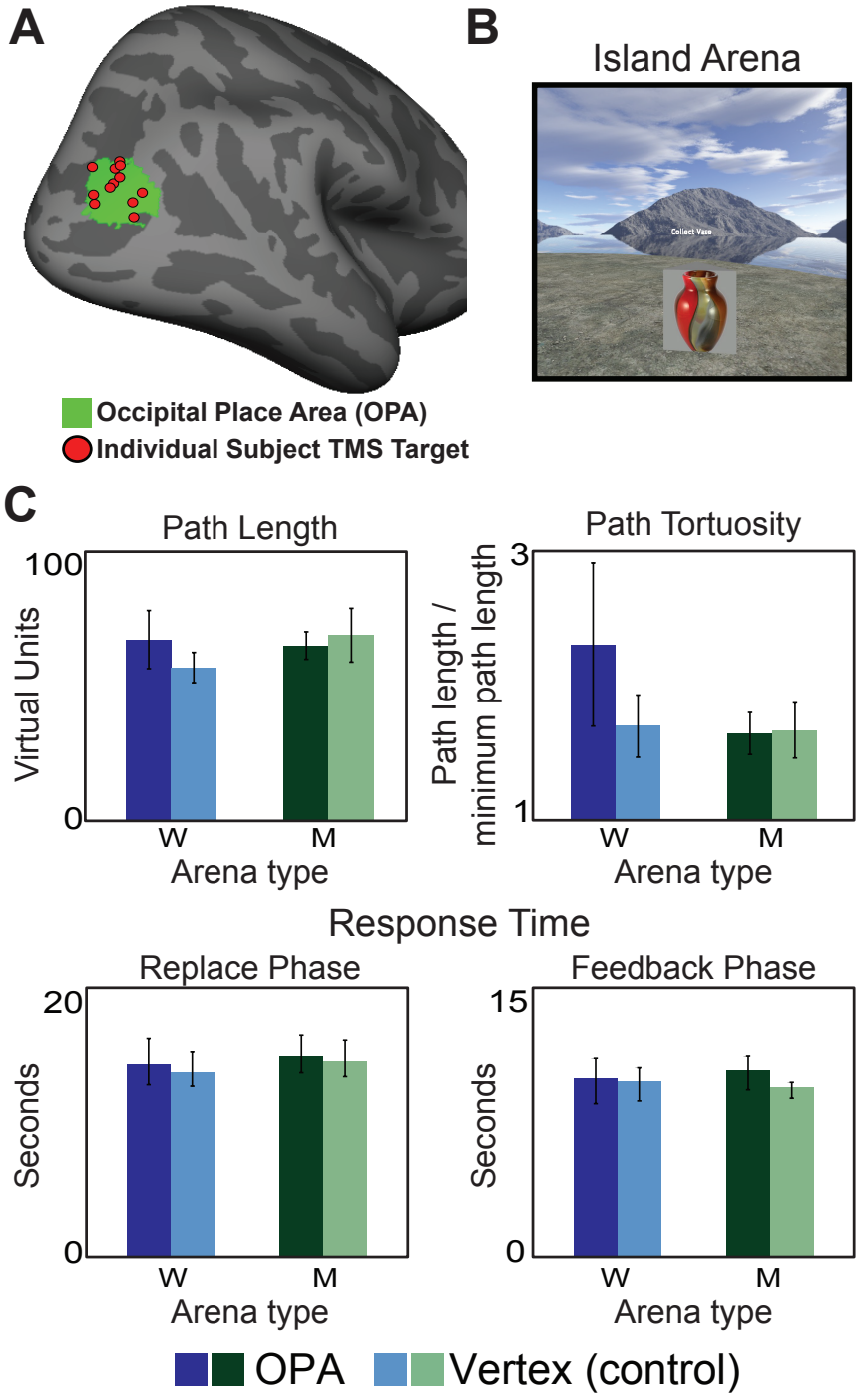

Figure S2. Supplemental Methods and Results for Experiment 2 (related to Figure 3). **A)** The group-based right Occipital Place Area (OPA) derived from a large number (42) of subjects across several studies from our laboratory, shown in green on the average cortical surface [S1]. The OPA TMS target site was defined for each participant as the OPA voxel exhibiting peak scene-selectivity. Each red dot denotes an OPA target site for a single participant in Experiment 2 (mean Talairach coordinates: [35, -79, 22]). **B)** In addition to the Wall and Mat Arenas, in Exp. 3 participants were also tested in the Island Arena. Data from the Island were inconclusive; see *Supplemental Experimental Procedures* for more information. **C)** Mean path length and path tortuosity during the replace phase, and mean response time during both the replace phase and feedback phase, separately for the OPA (dark colors) and Vertex (light colors) sessions for the Wall Arena (*W*; in blue) and Mat Arena (*M*; in green) (±1 SEM). Path tortuosity for each trial was computed as the path length divided by the Euclidean distance between the starting and end location of the path taken by the participant. Separate 2(arena: Wall vs. Mat) x 2(stimulation site: OPA vs. Vertex) ANOVAs revealed no significant main effects or interactions for path length, or response time during the replace or feedback phases (all $F(1,11)$s < 2.50, all ps > 0.14). Path tortuosity was marginally lower in the Mat than in the Wall Arena ($F(1,11)=3.62$, $p=0.08$), but critically there was no significant main effect of stimulation site or interaction (both $F(1,11)$s < 0.89, both ps > 0.35).

Table S1. Related to Figures 1 and 2. Complete results of the analyses of variance performed on data from blocks 2-3 of Experiment 1. Overall performance is analyzed in the top table and influence of the landmark in the bottom table. Significant effects ($p < 0.05$) are indicated in bold.

Performance

	df	F	Sig.	Partial Eta Squared
Object Type (Landmark-tethered vs. Boundary-tethered)	**1**	**7.086**	**.022**	**.392**
Stimulation Site (OPA vs. Vertex)	**1**	**14.755**	**.003**	**.573**
Block (2 vs. 3)	1	2.515	.141	.186
Trial (1-4)	**3**	**34.640**	**.000**	**.759**
Object Type * Stimulation Site	**1**	**10.144**	**.009**	**.480**
Object Type * Block	1	2.050	.180	.157
Stimulation Site * Block	1	.537	.479	.047
Object Type * Stimulation Site * Block	1	.223	.646	.020
Object Type * Trial	3	.680	.571	.058
Stimulation Site * Trial	3	1.127	.352	.093
Object Type * Stimulation Site * Trial	3	.937	.434	.078
Block * Trial	**3**	**3.120**	**.039**	**.221**
Object Type * Block * Trial	3	.250	.861	.022
Stimulation Site * Block * Trial	3	1.976	.137	.152
Object Type * Stimulation Site * Block * Trial	3	.127	.943	.011

Landmark Influence

	df	F	Sig.	Partial Eta Squared
Object Type (Landmark-tethered vs. Boundary-tethered)	**1**	**35.521**	**.000**	**.764**
Stimulation Site (OPA vs. Vertex)	**1**	**6.409**	**.028**	**.368**
Block (2 vs. 3)	1	.250	.627	.022
Trial (1-4)	3	2.029	.129	.156
Object Type * Stimulation Site	1	1.011	.336	.084
Object Type * Block	**1**	**12.809**	**.004**	**.538**
Stimulation Site * Block	1	1.011	.336	.084
Object Type * Stimulation Site * Block	1	.290	.601	.026
Object Type * Trial	**3**	**27.760**	**.000**	**.716**
Stimulation Site * Trial	3	.711	.552	.061
Object Type * Stimulation Site * Trial	3	2.503	.076	.185
Block * Trial	3	.714	.551	.061
Object Type * Block * Trial	**3**	**5.756**	**.003**	**.344**
Stimulation Site * Block * Trial	3	.729	.542	.062
Object Type * Stimulation Site * Block * Trial	3	2.632	.066	.193

Table S2. Related to Figure 3. Complete results of the analyses of variance performed on performance data from blocks 2-3 of Experiment 2. Significant effects ($p < 0.05$) are indicated in bold.

	df	F	Sig.	Partial Eta Squared
Arena (Wall vs. Mat)	1	0.252	.626	.022
Stimulation Site (OPA vs. Vertex)	1	0.119	.737	.011
Trial (1-3)	**2**	**5.476**	**.012**	**.332**
Arena * Stimulation Site	**1**	**5.971**	**.033**	**.352**
Arena * Trial	2	.548	.586	.047
Stimulation Site * Trial	2	.398	.676	.035
Arena * Stimulation Site * Trial	2	.548	.586	.047

Supplemental Experimental Procedures

Participants. Two groups of twelve participants gave written consent and were paid for participating in Exp. 1 (5 female, mean age 23, age range 20-28) and Exp. 2 (4 female, mean age 24, age range 19-33). Five subjects participated in both experiments, separated by roughly six months. All had normal or corrected-to-normal vision and reported to be in good health with no history of neurological disease. All subjects provided informed consent in accordance with the Institutional Review Board of the University of Pennsylvania.

fMRI Localization of the OPA. Prior to TMS, each participant completed an fMRI localizer scan to localize the right OPA. Scanning was performed at the Hospital of the University of Pennsylvania using a 3T Siemens Trio scanner equipped with a 32-channel head coil. High-resolution T1-weighted images for anatomical localization were acquired using a three-dimensional magnetization-prepared rapid acquisition gradient echo pulse sequence [repetition time (TR), 1620 ms; echo time (TE), 3.09 ms; inversion time, 950 ms; voxel size, 1 x 1 x 1 mm; matrix size, 192 x 256 x 160]. T2*-weighted images sensitive to blood oxygenation level-dependent contrasts were acquired using a gradient echo echoplanar pulse sequence (TR, 3000 ms; TE, 30 ms; flip angle 90°; voxel size, 3 x 3 x 3 mm; field of view, 192; matrix size, 64 x 64 x 44). Visual stimuli were displayed by rear-projecting them onto a Mylar screen at 1024 x 768 pixel resolution with an Epson 8100 3-LCD projector equipped with a Buhl long-throw lens. Subjects viewed the images through a mirror attached to the head coil.

During scanning, subjects completed two functional localizer scans. The localizer procedure was identical to the procedure used in prior reports (e.g, [S2]) These scans were each 5 min 21 s in length, during which subjects performed a 1-back repetition detection task on color images of faces, scenes, objects, and scrambled objects, presented in 16 s blocks with each stimulus shown for 600 ms each with a 400 ms interstimulus interval. Images subtended a visual angle of approximately 9.0° x 9.0°.

Data from the localizer scans were analyzed with the FMRIB Software Library (FSL) using the following steps. First, they were corrected for differences in slice timing by resampling slices in time to match the first slice of each volume. Second, they were corrected for subject motion by realigning to the first volume of the scan run using MCFLIRT [S3]. Third, the timecourses for each voxel were high-pass filtered to remove low temporal frequency fluctuations in the BOLD signal that exceeded lengths of 100 s. Data were then spatially smoothed with a 5 mm full-width at half-maximum Gaussian filter. A GLM consisting of a boxcar regressor convolved with a standard double gamma function was then used to model the fMRI response to each stimulus condition. The scene-selective right OPA was identified in each participant by overlaying individual scenes > objects contrast maps on high-resolution MRI scans for each participant. The anatomical location of the right OPA, near the transverse occipital and intraparietal sulci, was confirmed using standard methods [S1] (Figures S1A and S2A).

Stimulation Sites and Transcranial Magnetic Stimulation. The Brainsight system (Rogue Research, Montreal) was used to co-register MRI data with the location of the subject and the TMS coil. The OPA stimulation site was defined in each participant by selecting the voxel exhibiting peak scene-selectivity (i.e., the highest t-value from the scenes > objects contrast) in the right OPA. The Vertex control site was identified in each participant as the midpoint between the bridge of the nose and the inion, and between the temples. A Magstim Super Rapid^2 Plus^1 stimulator (Magstim; Whitland, UK) was used to deliver cTBS via a 70 mm diameter figure-eight coil. For OPA stimulation, the TMS coil handle was held pointing upwards. To calibrate the intensity of stimulation, cTBS was delivered at 80% of each participant's phosphene threshold. Each participant's phosphene threshold was determined prior to the start of the first experimental session using a standard up-down staircase procedure with stimulation to visual area V1 [S4].

For both experiments, each subject participated in two testing sessions separated by one week, one for each of the two stimulation sites (counterbalanced across subjects). In Exp. 1, stimulation was applied immediately prior to each testing block, and in Exp. 2 stimulation was applied five minutes prior to each testing block.

Virtual Reality Environments and Testing Procedure. We used Source SDK Hammer Editor (http://www.valvesoftware.com, Valve Software, Bellevue, WA) to construct a virtual reality environment that was rendered and displayed from the first person-perspective using the commercial game software Portal (http://www.valvesoftware.com, Valve Software, Bellevue, WA). The environment was displayed on a 27-inch LG monitor (resolution: 1920 x 1080) and participants were seated roughly 50 cm from the screen. In both experiments, participants learned the locations of target objects inside an arena in the virtual environment, using the learning procedure illustrated in Figure 1A. Participants moved through the arena by using their right hand to operate arrow keys to move forward or backwards and turn left or right. Responses during the replace phase were collected by participants pressing the "e" key with their left hand. Virtual heading and location were recorded every 100 ms.

In Exp. 1, participants were tested inside an arena consisting of a landmark object surrounded by a circular boundary

wall. The boundary wall was 130 virtual units (vu) in diameter, and 10 vu in height relative to a simulated eye-level of 4 vu. One virtual unit corresponds to 0.3048 real-world meters (1 foot). The landmark object was either a trashcan or a metal ball, counterbalanced across TMS target sites. The complete set of target objects was either [coffee table, propane tank, barrel, traffic cone] or [radiator, lamp, oil drum, cake], counterbalanced across TMS target sites. The target objects for each trial were selected in pseudo-random order. Prior to the start of the first replace phase during block 1, but not blocks 2-3, participants collected each target object in pseudo-random order twice (i.e., performed the feedback phase twice per target object) in order to learn the locations of the objects.

In Exp. 2, participants were tested in two different circular arenas: Wall and Mat. The Wall Arena surrounded by a wall as in Exp. 1. The Mat Arena consisted of a visual texture (or "mat") drawn on the ground. Both the Wall and Mat arenas had the same visual texture drawn on the ground; thus, the Wall and Mat arenas were visually identical except for the presence of the boundary. The Wall and Mat Arenas had the same diameter as the Exp. 1 arena. The boundary wall in the Wall Arena was 4 vu in height, which is shorter than the boundary wall in Exp. 1 so that the visibility of the distal cues were better matched between the Wall and Mat Arenas. Participants could walk beyond the edge of the mat in the Mat Arena, and were instructed that they could do so. However, participants only spent an average of 4.7% of the total testing time beyond the edge of the mat, and there was no difference in time spent outside the mat edge between the OPA and Vertex sessions ($t(11)= 0.20$, $p > 0.5$). The complete set of target objects in the Wall Arena was either [basketball, hairdryer, arm chair, refrigerator] or [cooler, binoculars, computer monitor, hat]. The complete set of target objects in the Mat Arena was either [washer, calculator, bench, cabinet] or [vacuum, bowling ball, cell phone, stapler]. Target object sets were counterbalanced across TMS target sites for each arena. The target objects for each trial were selected in pseudo-random order. Prior to the start of the first replace phase in each arena, participants collected each target object in pseudo-random order twice (i.e., performed the feedback phase twice per target object).

In addition to the Wall and Mat Arenas in Exp. 2, participants were also tested in a third arena: the Island (Figure S2B). The Island consisted of a circular island surrounded by "water" that impeded movement. This arena was included to examine if the OPA codes boundaries defined solely by their impediment to movement, and not just surface boundaries. Prior to testing in the Island arena, participants were informed that they could not walk beyond the island edge. The complete set of target objects in the Island Arena were [bottle, piano, football, coffee maker] or [treadmill, vase, soccer ball, sofa], counterbalanced across TMS target sites. In the Island, we observed no difference in overall performance between the OPA and Vertex sessions ($t(11)=0.10$, $p > 0.5$). However, performance in this arena was confounded with response time: participants took significantly more time to replace the objects following OPA stimulation than after stimulation of Vertex ($t(11) = 2.36$, $p < 0.05$). Further, 10 out of 12 participants took longer to collect the target objects during the feedback phase following OPA stimulation compared to Vertex ($p < 0.05$, sign-test), although one participant went strongly in the opposite direction. Thus, results from this experiment were ambiguous: on the one hand, the absence of an accuracy difference suggests that OPA might *not* be involved in processing boundaries that are defined by an obstacle at ground level rather than a wall; on the other hand, the fact that response times were longer after OPA stimulation suggests that an impairment in accuracy may have been masked by a speed-accuracy tradeoff. Because of the ambiguity of the results, data from the Island were omitted from further analyses.

Supplemental References

S1. Julian J., Fedorenko E., Webster J., & Kanwisher N. (2012). An algorithmic method for functionally defining regions of interest in the ventral visual pathway. Neuroimage *60*, 2357-2364.

S2. Marchette S.A., Vass L.K., Ryan J., & Epstein R.A. (2015). Outside Looking In: Landmark Generalization in the Human Navigational System. The Journal of Neuroscience *35*, 14896-14908.

S3. Jenkinson M., Bannister P., Brady M., & Smith S. (2002). Improved optimization for the robust and accurate linear registration and motion correction of brain images. Neuroimage *17*, 825-841.

S4. Kammer T. & Beck S. (2002). Phosphene thresholds evoked by transcranial magnetic stimulation are insensitive to short-lasting variations in ambient light. Experimental brain research *145*, 407-410.